Replica Exchange for Reactive Monte Carlo Simulations†

C. Heath Turner*

Department of Chemical and Biological Engineering, University of Alabama, Tuscaloosa, Alabama 35487-0203

John K. Brennan

U.S. Army Research Laboratory, Weapons and Materials Research Directorate, Aberdeen Proving Ground, Maryland 21005-5066

Martin Lísal

E. Hála Laboratory of Thermodynamics, Institute of Chemical Process Fundamentals, Academy of Sciences of the Czech Republic, 165 02 Prague 6-Suchdol, Czech Republic and Department of Physics, Faculty of Science, J.E. Purkinje University, 400 96 Ústí nad Labem, Czech Republic

Received: April 4, 2007; In Final Form: July 9, 2007

A new application of the replica exchange technique is demonstrated for use in reactive Monte Carlo simulations. The technique allows the system to traverse barriers in the free energy landscape through configuration swaps of higher temperature replicas, replicas with scaled potential energy parameters, or replicas existing at modified values of the reaction driving force (free energy of reaction). Acceptance rules are derived for the swap moves among the replicas, and the application of the replica exchange method is shown to be straightforward. We demonstrate the accuracy and efficiency of this technique by simulating the conversion of a model reaction. We find large increases in efficiency when performing simulations at computationally challenging conditions, such as high densities, particularly when a preconverged configuration reservoir is incorporated. It is possible to extend this replica exchange approach to systems involving multiple simultaneous reactions and to systems with more complex multisite reacting species.

1. Introduction

There has been growing interest in the replica exchange simulation technique during the past few years.[1,2] The central theme of the technique is to create multiple replicas of the central image, with each replica corresponding to a slightly different set of simulation parameters, and during the course of the simulation, configurations are periodically exchanged between the different replicas, according to a Metropolis acceptance criteria. The parameters that are varied among the replicas are intended to increase sampling efficiency by allowing the central image to quickly escape local minima traps. Replica exchange has been applied to various ensembles, such as the canonical ensemble (where the temperature is often used as the index parameter),[2−4] the grand canonical ensemble (where the chemical potential or temperature can be used as the index parameter),[5,6] and the microcanonical ensemble.[7] Also, it has been used in the *q*-jumping Monte Carlo method,[8] the Hamiltonian replica exchange method,[9,10] and the resolution exchange method.[11]

Here, we present a further application of the replica exchange technique, formulated for use in reactive Monte Carlo (RxMC) simulations.[12,13] RxMC simulations can be used to predict the equilibrium conversions of chemical reactions in various nonideal environments.[14−28] The primary inputs are the intermolecular potentials and the standard free energy of the reactions in an ideal gas reference state. However, the efficiency of standard RxMC simulations can be degraded by a number of factors, including high densities, strong intermolecular interactions, or low temperatures. This is due to the fact that the forward and reverse reaction steps involve insertions and deletions of molecules in the fluid, and these moves have very low acceptance probabilities in these cases, similar to the challenges of grand canonical simulations. To overcome such challenges, we have adapted the replica exchange method within the RxMC framework. This idea was introduced several years earlier by Escobedo[29] but is only now being implemented here for the first time. Replicas within the replica exchange RxMC method (RE-RxMC) can exist at incremental values of the temperature, the intermolecular potential energy, the volume, or the ideal reaction free energy changes ($\Delta G°$). We have invested minimal effort into optimizing the various factors which govern the efficiency of the method, such as the number of replicas used or the spacing between the replicas. Rather, our primary goal was to demonstrate the accuracy of this approach by performing simulations at mild conditions, followed by additional simulations at challenging conditions, in order to evaluate the relative efficiency of this technique. In the following sections, we demonstrate the accuracy and the relative efficiency of this technique for a reaction of the form $2R \leftrightarrow P$, at several different ideal (low density) and nonideal (high density) conditions. The replica exchange technique is found to significantly increase the sampling of the forward and reverse reaction moves at high densities, greatly improving the convergence to the equilibrium reaction conversion (which is the typical quantity of interest). We also find that it is particularly beneficial to

† Part of the "Keith E. Gubbins Festschrift".

* Corresponding author.

10.1021/jp072655t CCC: $37.00
Published on Web 08/16/2007

incorporate a preconverged image reservoir,[30,31] especially if there is a reasonable estimate of the average reaction conversion of the system a priori.

As with most other advanced sampling techniques, the efficiency of the replica exchange method is sensitive to the particular conditions being simulated, and so we intend to identify the tradeoff between the cost of the implementation and the expected efficiency gained for RE-RxMC simulations. First, it is important to recognize that at computationally mild conditions, the additional replicas may actually decrease the overall performance of the simulation, since the total number of Monte Carlo (MC) moves in a given simulation must be distributed among the collection of replicas. In other words, some systems may actually equilibrate more quickly or sample phase space more efficiently if the central image is simulated exclusively (i.e., standard RxMC simulations), where all of the simulation effort is focused on this one image. The diminishing performance of the replica exchange technique has also been observed by others in cases where the free energy barriers in the system are small.[32] Therefore, this technique is most useful for extending the applicability of the RxMC method beyond traditional simulation limits, such as strongly associating fluids and high-density fluids. A thorough discussion of the benefits and challenges of the replica exchange technique is given by Okur and co-workers,[30] as well as the motivation for incorporating a preconverged structure reservoir, which we have used here. As noted previously by others,[6] the replica exchange approach can be considered as an arbitrary (but correct) method for initiating fluctuations in phase space, in order to enhance sampling efficiency.

2. Exchange Criteria for RxMC Simulations. The Monte Carlo moves within each individual replica follow the standard RxMC simulation protocol.[12,13] The attempted moves are particle displacement/reorientation and forward/reverse reaction steps, with the acceptance probabilities given respectively as

(i) molecule displacement/reorientation,

$$P_{\text{acc}} = \min[1, \exp(-\beta\Delta U)] \tag{1}$$

and (ii) forward/reverse reaction step,

$$P_{\text{acc}} = \min\left[1, \exp(-\beta\Delta U)\prod_{i=1}^{C}(q_i V)^{\xi\nu_i}\prod_{i=1}^{C}\frac{N_i!}{(N_i+\xi\nu_i)!}\right] \tag{2}$$

where eq 2 is written for a single reaction; that is, $\sum_{i=1}^{C}\nu_i S_i = 0$. The symbol ν_i represents the stoichiometric coefficient of each species S_i and is defined to be negative for reactants and to be positive for products. In the equations above, β is the reciprocal of the Boltzmann constant times the absolute temperature, $(k_B T)^{-1}$, C represents the number of species in the reaction, V is the volume of the system, N_i is the number of molecules of species i, ξ is the extent of reaction, and ΔU is the change in the configurational energy for the displacement/reorientation or forward/reverse reaction step. The symbol q_i represents the internal partition function corresponding to an isolated molecule of species i, where $q_i = q_{i,\text{rot}} \times q_{i,\text{vib}} \times q_{i,\text{e}}/\Lambda_i^3$. Here, $q_{i,\text{rot}}$, $q_{i,\text{vib}}$, $q_{i,\text{e}}$, and Λ_i represent the rotational, vibrational, and electronic partition functions and the de Broglie thermal wavelength, respectively.

Now, in order to generate the acceptance rules for performing configuration swaps among the replicas, we begin with the formalism used by Yan and de Pablo.[6] Accordingly, we begin from a generalized ensemble, which is defined by the partition function $Z(\mathbf{f})$.

$$Z(\mathbf{f}) = \sum_x \Omega(x) w(x,\mathbf{f}) \tag{3}$$

The generalized forces or potentials defining the thermodynamic state of the system are represented by the $\mathbf{f}$ vector, $\Omega(x)$ is the density of states, and $w(x,\mathbf{f})$ is the weighting function for configuration x with generalized potentials $\mathbf{f}$. With regards to an RxMC ensemble, the $\mathbf{f}$ vector can be defined by the temperature (T), the chemical potential of the components (μ_i), and the internal partition function of the reacting species (q_i). Therefore, the weighting function for the RxMC ensemble can be expanded into the following form:[12,13]

$$w(x,\mathbf{f}) = \exp\{\beta\sum_{i=1}^{C}N_i(x)\mu_i - \sum_{i=1}^{C}\ln[N_i(x)!] + \sum_{i=1}^{C}N_i(x)\ln[q_i V] - \beta U(x)\} \tag{4}$$

In the above expression, $N_i(x)$ is the total number of molecules of species i in configuration x and $U(x)$ is the potential energy of configuration x. With these definitions, we can examine a collection of M noninteracting replicas, which is specified by the partition function $Z(\mathbf{f}_i)$. We define our collection of replicas so that replica 1 corresponds to the central image and replica M corresponds to the last replica. The total partition function for this collection of M replicas, Z_c, is given by eq 5, and the unnormalized probability density of the composite state $\mathbf{x}$ is shown in eq 6.

$$Z_c(\mathbf{f}_1,\mathbf{f}_2,\ldots\mathbf{f}_M) = \prod_{i=1}^{M} Z(\mathbf{f}_i) \tag{5}$$

$$p(\mathbf{x}) = \prod_{i=1}^{M}\Omega(x_i)w(x_i,\mathbf{f}_i) \tag{6}$$

As applied to RxMC simulations, these replicas constitute individual, reacting systems at chemical equilibrium, distributed according to the probability $p(\mathbf{x})$. Translation of this theoretical framework into a simulation protocol to be used in RE-RxMC is a relatively simple task. In addition to the standard RxMC simulation moves performed within each replica, attempts are also made to exchange configurations among the replicas. We randomly pick a pair of neighboring replicas (here, labeled A and B) and attempt to swap the configuration of these replicas with the following acceptance probability:

$$p_{\text{acc}}(x_A \leftrightarrow x_B) = \min\left[\frac{w(x_B,\mathbf{f}_A)w(x_A,\mathbf{f}_B)}{w(x_A,\mathbf{f}_A)w(x_B,\mathbf{f}_B)}\right] \tag{7}$$

The individual terms contained in eq 7 can be expanded as shown below.

$$w(x_B,\mathbf{f}_A) = \exp\{\beta_A\sum_{i=1}^{C}N_i(x_B)\mu_{iA} - \sum_{i=1}^{C}\ln[N_i(x_B)!] + \sum_{i=1}^{C}N_i(x_B)\ln[q_{iA}V_A] - \beta_A U_A(x_B)\} \tag{8}$$

$$w(x_A,\mathbf{f}_B) = \exp\{\beta_B \sum_{i=1}^{C} N_i(x_A)\mu_{iB} - \sum_{i=1}^{C} \ln[N_i(x_A)!] + \sum_{i=1}^{C} N_i(x_A) \ln[q_{iB}V_B] - \beta_B U_B(x_A)\} \quad (9)$$

$$w(x_A,\mathbf{f}_A) = \exp\{\beta_A \sum_{i=1}^{C} N_i(x_A)\mu_{iA} - \sum_{i=1}^{C} \ln[N_i(x_A)!] + \sum_{i=1}^{C} N_i(x_A) \ln[q_{iA}V_A] - \beta_A U_A(x_A)\} \quad (10)$$

$$w(x_B,\mathbf{f}_B) = \exp\{\beta_B \sum_{i=1}^{C} N_i(x_B)\mu_{iB} - \sum_{i=1}^{C} \ln[N_i(x_B)!] + \sum_{i=1}^{C} N_i(x_B) \ln[q_{iB}V_B] - \beta_B U_B(x_B)\} \quad (11)$$

These terms can then be combined into a single expression for the acceptance criteria by substituting them into eq 7 and then grouping similar terms together:

$$p_{acc} = \min\{1, \exp\{\beta_A \sum_{i=1}^{C} N_i(x_B)\mu_{iA} + \beta_B \sum_{i=1}^{C} N_i(x_A)\mu_{iB} - \beta_A \sum_{i=1}^{C} N_i(x_A)\mu_{iA} - \beta_B \sum_{i=1}^{C} N_i(x_B)\mu_{iB} - \sum_{i=1}^{C} \ln[N_i(x_B)!] - \sum_{i=1}^{C} \ln[N_i(x_A)!] + \sum_{i=1}^{C} \ln[N_i(x_A)!] + \sum_{i=1}^{C} \ln[N_i(x_B)!] + \sum_{i=1}^{C} N_i(x_B) \ln[q_{iA}V_A] + \sum_{i=1}^{C} N_i(x_A) \ln[q_{iB}V_B] - \sum_{i=1}^{C} N_i(x_A) \ln[q_{iA}V_A] - \sum_{i=1}^{C} N_i(x_B) \ln[q_{iB}V_B] - \beta_A U_A(x_B) - \beta_B U_B(x_A) + \beta_A U_A(x_A) + \beta_B U_B(x_B)\}\} \quad (12)$$

In order to simplify the above expression, we group the terms in the exponential function (according to each line of the equation) and define these as I, II, III, and IV, respectively, so that the acceptance probability becomes

$$p_{acc} = \min\{1, \exp[(I) + (II) + (III) + (IV)]\} \quad (13)$$

At this point, we simplify each of the terms, I−IV, beginning with term I. First, we introduce the symbol $\delta\xi$, which can be used to account for the difference in the extent of conversion among the two replicas.

$$\delta\xi = \frac{N_i(x_B) - N_i(x_A)}{\nu_i} \quad (14)$$

Now, term I can be written more compactly as

$$(I) = +\beta_A \delta\xi \sum_{i=1}^{C} \nu_i\mu_{iA} - \beta_B \delta\xi \sum_{i=1}^{C} \nu_i\mu_{iB} \quad (15)$$

The relationship between the chemical potentials within each replica obeys the following requirement for chemical equilibrium:

$$\sum_{i=1}^{C} \nu_i\mu_i = 0 \quad (16)$$

Upon substitution of these equalities, it is found that expression I becomes 0. The next term in eq 13, labeled II, likewise reduces to 0, so we now focus on the third term. This term can be simplified and reduced into a more compact expression by again introducing the symbol $\delta\xi$.

$$(III) = \ln\left[\left(\prod_{i=1}^{C}\left(\frac{q_{iA}V_A}{q_{iB}V_B}\right)^{\nu_i}\right)^{\delta\xi}\right] \quad (17)$$

This expression can be further simplified, if we introduce a new variable, ΔG_i°, which represents the ideal gas standard free energy (at reference pressure P°) of the reaction within replica i. The relationship between the partition functions and the free energy of reaction found in standard thermodynamic tables[33] is defined as:[34]

$$\prod_{j=1}^{C} q_j^{\nu_j}\left(\frac{RT_i}{P^\circ}\right)^{\nu_j} = \exp(-\Delta G_i^\circ/RT_i) \quad (18)$$

In the above equation, R is the ideal gas constant. If the free energy of reaction is substituted into eq 17, then term III can be rewritten as

$$(III) = \ln\left[\left(\frac{\exp(-\Delta G_A^\circ/RT_A)}{\exp(-\Delta G_B^\circ/RT_B)}\right)^{\delta\xi}\left(\frac{P^\circ V_B}{RT_B}\right)^{\delta\xi}\left(\frac{RT_A}{P^\circ V_A}\right)^{\delta\xi}\right] = \delta\xi\left[-\left(\frac{\Delta G_A^\circ}{RT_A} - \frac{\Delta G_B^\circ}{RT_B}\right) + \ln\left(\frac{V_B T_A}{V_A T_B}\right)\right] \quad (19)$$

The last term in eq 13, IV, can be simplified as shown below with the definitions: $\Delta U_i(x_{ij}) = [U_i(x_i) - U_i(x_j)]$ and $\beta_i = 1/(k_B T_i)$, where the $U_i(x)$ term represents the potential energy of configuration x calculated with the intermolecular potential assigned to replica i.

$$(IV) = -\beta_A \Delta U_A(x_{BA}) - \beta_B \Delta U_B(x_{AB}) \quad (20)$$

Combining all of the partial expressions (I−IV) yields the final result:

$$p_{acc} = \min\left\{1, \exp\left[-\beta_A \Delta U_A(x_{BA}) - \beta_B \Delta U_B(x_{AB}) - \delta\xi\left(\frac{\Delta G_A^\circ}{RT_A} - \frac{\Delta G_B^\circ}{RT_B}\right) + \delta\xi \ln\left(\frac{V_B T_A}{V_A T_B}\right)\right]\right\} \quad (21)$$

In all of the simulations reported here, we are working in the canonical ensemble so that the temperatures and volumes are identical in all replicas. However, the intermolecular potential and the free energy of reaction are allowed to vary among the replicas. Therefore, for our current simulations, the relevant swap acceptance probability becomes

$$p_{acc} = \min\left\{1, \exp\left[-\beta(\Delta U_A(x_{AB}) + \Delta U_B(x_{BA})) - \delta\xi\left(\frac{\Delta G_A^\circ - \Delta G_B^\circ}{RT}\right)\right]\right\} \quad (22)$$

The above expression is valid for a single reaction with constant volume replicas, and it will be applied to the test reaction simulated in the present study: $2R \leftrightarrow P$.

TABLE 1: Intermolecular Parameters for the Reactant and Product in the 2R ↔ P Model Reaction[a]

molecule	site #	ϵ_i/ϵ_R	σ_i/σ_R	z_i	bl/σ_R
R	1	1.00	1.00		
P	1	0.50	1.40	+0.30	0.50
	2	0.50	1.40	−0.30	0.50

[a] Symbol '*bl*' represents the site distance from the geometric molecular center

An RE-RxMC simulation in the canonical ensemble is initiated by specifying the initial composition, volume, and temperature of the central replica, along with the intramolecular partition functions (or free energy of reaction) and the intermolecular potentials. The neighboring replicas are all initiated in the same way, except that the temperature, the free energy of the reaction, the potential energy parameters, or the volume may be scaled. The parameter spacing among the replicas and the total number of replicas can be optimized to enable efficient sampling of phase space. However, we have not pursued the optimization of the various replica exchange parameters in detail since these will depend upon the particular system being simulated. Others have explored routes for achieving optimal parameters in other replica exchange applications, suggesting that an efficiency maximum can be achieved with a replica swap acceptance of between 20 and 40%.[35,36]

3. Models and Simulation Details. To demonstrate and verify the accuracy of the RE-RxMC approach, we first modeled the nonspecific reaction, 2R ↔ P, at computationally mild conditions (low density, high temperature) and thus provided a benchmark for which to compare results at computationally challenging conditions. Interactions between molecule *i* and molecule *j* were modeled using the Lennard-Jones (LJ) potential plus electrostatic point charges, according to the following form:

$$u_{ij} = \sum_{\alpha}\sum_{\beta} 4\epsilon_{i\alpha,j\beta}\left[\left(\frac{\sigma_{i\alpha,j\beta}}{r_{i\alpha,j\beta}}\right)^{12} - \left(\frac{\sigma_{i\alpha,j\beta}}{r_{i\alpha,j\beta}}\right)^{6}\right] + \frac{z_{i\alpha}z_{j\beta}}{r_{i\alpha,j\beta}} \quad (23)$$

In eq 23, the calculation is summed over sites α on molecule *i* and sites β on molecule *j*. The site−site separation distance is *r*; *z* represents the electrostatic charge assigned to each site, and ϵ and σ are the LJ parameters for each site. A potential cutoff distance of $5\sigma_R$ was used for both electrostatic and LJ interactions. Beyond this distance, long-range corrections were used for the LJ potential, and the site−site reaction field method[37] was used to account for the long-range electrostatic interactions.

The intermolecular parameters assigned to R and P are listed in Table 1. Molecule R is a spherical LJ molecule and molecule P is a LJ diatomic with two point charges. The free energy of the reaction of the central image was chosen to be $\Delta G_1^\circ = -25.0$ (defined in reduced units, with respect to ϵ_R). The particular value of ΔG_1° was chosen arbitrarily but chosen as such to avoid the extremes of 0 or 100% conversion and result in moderate conversions at the conditions studied. The model reaction and system parameters are for demonstration purposes only, and we do not ascribe any particular physical relevance to this system. If a specific reaction was being modeled, the intermolecular parameters and the free energy of reaction would need to be precisely obtained, corresponding to the experimental system. However, in this work, the main intent is to verify the accuracy and quantify the efficiency of the RE-RxMC method versus the standard RxMC protocol by exploring several different state points.

All simulations were initiated by placing the molecules on a cubic lattice, with a lattice spacing corresponding to the specified density. On average, each MC step was attempted with the following frequencies: displacement/reorientation (59%), configuration swap (1%), forward reaction step (20%), and reverse reaction step (20%). The number of steps to achieve equilibration varied, as well as the total length of the run, but a typical simulation at low density took 10×10^6 moves for equilibration, followed by 50×10^6 moves for averaging, whereas the high-density conditions often required more than 1000×10^6 total MC moves. On a single-processor machine, the low-density simulations equated to approximately 2 h of wall clock time, and the high-density simulations required ~3 days/1000×10^6 MC moves for our system of 768 interaction sites ($N_R + 2N_P$). Statistics from the simulations were generated by dividing each of the simulation runs into 10 blocks, which were then used to calculate the standard deviations of the reported averages.

Following initial tests of the reaction at low densities and high temperatures, we explored more computationally challenging conditions (lower temperatures and higher densities). While the first set of simulations was used to validate the accuracy and reliability of the RE-RxMC technique, the next set of simulations was chosen to serve as a test bed for evaluating the relative efficiency of the replica exchange technique. At each of these conditions, we compared the equilibrium conversion of the reaction, the average potential energy, and the average pressure. Also, an important measure of the equilibration and sampling efficiency in these simulations is the total number of accepted forward and reverse reaction steps. In standard RxMC simulations, the number of forward and reverse reaction steps can be monitored in a straightforward manner, since only one complete forward or reverse reaction step can potentially be sampled during each MC step. However, when the replica exchange moves are implemented, successful configuration swaps can effectively shift the conversion of the replicas, since the mole fractions of the two replicas are not necessarily equal. We incorporated this effective conversion shift when counting the total number of successful forward and reverse reaction steps in the RE-RxMC simulations. Accordingly, when a replica swap is accepted, the difference in conversions between the replicas is related to the number of forward or reverse reaction steps needed to change the conversion of the original configuration to its newly adopted configuration (equivalent to the $\delta\xi$ parameter defined earlier in eq 14). In other words, there is often a shift in the mole fraction during a replica exchange move, and this shift is accounted for when we count the total number of successful forward and reverse reaction steps of a particular image.

To improve sampling efficiency, the replicas were chosen to adopt a scaled form of the intermolecular potential by incorporating the κ parameter ($\kappa \leq 1$), where $u_{ij} = \kappa \times u_{ij}$ in order to "soften" the potential of the neighboring replicas. As the magnitude of the potential energy is reduced, the number of successful forward and reverse reaction steps in the replicas can be greatly increased, and the sampling of the equilibrium conversion can therefore be improved. As $\kappa \rightarrow 0$, the ideal gas limit is approached, and the conversion in the simulation can be checked against an analytical calculation. While forward and reverse reactions can be easily performed in the low density and high-temperature simulations, the reactions become relatively rare events at high density and low-temperature conditions in standard RxMC simulations, thus motivating our RE-RxMC procedure.

Since the replica configurations are periodically exchanged, the central image is allowed to explore the different reaction conversions existing in the neighboring replicas, without ever

TABLE 2: Validation of the Replica Exchange Technique against Standard RxMC Simulations for the Reaction 2R ↔ P[a]

ρ_T*	T*	M	N_R	N_P	x_P	U*	P*
0.01	10.0	1	299.2(1)	234.4(1)	0.439	−1.095(3)	0.102(1)
		11	299.8(6)	234.1(3)	0.439	−1.092(3)	0.102(3)
		31	299.4(10)	234.3(5)	0.439	−1.098(26)	0.107(12)
	5.0	1	662.7(5)	52.7(2)	0.074	−0.301(4)	0.070(0)
		11	662.8(6)	52.6(3)	0.074	−0.297(4)	0.070(1)
		31	663.4(13)	52.3(6)	0.073	−0.290(11)	0.071(6)
0.10	10.0	1	63.5(1)	352.2(1)	0.847	−13.98(2)	0.905(22)
		11	63.5(3)	352.3(1)	0.847	−13.98(4)	0.909(6)
		31	63.6(5)	352.2(3)	0.847	−13.97(4)	0.904(11)
	5.0	1	87.5(3)	340.3(1)	0.795	−18.33(4)	0.176(12)
		11	87.8(8)	340.1(4)	0.795	−18.33(5)	0.167(9)
		31	87.7(17)	340.1(8)	0.795	−18.31(14)	0.168(8)
0.20	10.0	1	42.6(2)	362.7(1)	0.895	−21.38(4)	3.98(4)
		11	43.0(6)	362.5(3)	0.894	−21.35(6)	3.99(3)
		31	42.4(5)	362.8(3)	0.895	−21.42(14)	3.99(4)
	5.0	1	37.0(5)	365.5(2)	0.908	−27.80(4)	1.12(2)
		11	36.7(3)	365.7(2)	0.908	−27.82(3)	1.12(4)
		31	36.9(18)	365.6(9)	0.908	−27.82(19)	1.16(6)

[a] Numbers in parentheses represent one standard deviation of the last digit.

accepting a single forward/reverse reaction event in the central image. However, it is very important to recognize that (particularly at the high density and low-temperature conditions), since the potential energy is being significantly modified, there can be large deviations in the equilibrium conversion between the central image and the neighboring replicas. We found that if the conversions among two replicas differ by more than 1−2%, successful exchanges become relatively rare events. Ideally, the replicas (with the scaled potential) would only increase the sampling efficiency but otherwise result in a conversion very close to the equilibrium conversion corresponding to the full potential (i.e., the central image). In this way, there would be close configurational correspondence among the replicas, resulting in significant overlap among the replica Hamiltonians and thus increasing the exchange acceptance probability for the attempted swap moves.

To help mitigate any net shifts in the conversion among the replicas in the high density and low-temperature simulations, the softening of the potential can be balanced by an adjustment to the value of the reaction free energy (ΔG_i°), which strongly influences the conversion within each replica. If a softer potential pushes the conversion in a particular direction, the reaction free energy can be scaled to offset this shift. If an appropriate balance between these two parameters is found, the result is a collection of replicas that allows an increased number of forward and reverse reaction steps as well as larger maximum displacements/reorientations (due to the scaled potential), while simultaneously sampling conversions representative of the central replica (due to the scaled ΔG_i° value). We explain the choice of our particular replica exchange parameter values in the following section.

4. Results and Discussion

A. Accuracy: Low-Density Reacting Mixture. We began the verification procedure by choosing several state points at high temperature and moderate densities that would allow a standard RxMC simulation to equilibrate within a reasonable amount of computational time. The state points that we explored in the first set of simulations are listed in Table 2, along with the results from the standard RxMC simulations ($M = 1$) and the RE-RxMC simulations ($M = 11$ and 31), where M is the total number of replicas in the simulation (including the central image). Here, the repulsive interaction among the replicas varied by increments of $\delta\kappa = -0.03$, so that the last replica corresponds to a potential energy of $U_M(x) = [1 + (M - 1) \times (\delta\kappa)] \times U(x)$, where $U(x)$ is the full potential energy calculated according to eq 23. Here, in the low density and high-temperature case, shifts to the ideal gas driving force were not needed, since the potential energy shift did not induce any significant differences in the reaction equilibria among the replicas. However, if needed, the incremental difference of the reaction free energy among the replicas is defined so that the last replica corresponds to a reaction free energy of $\Delta G_M^\circ = \Delta G_1^\circ + (M - 1) \times (\delta\Delta G_{AB}^\circ)$.

The results in Table 2 show accurate performance of the RE-RxMC technique, as the equilibrium values of the conversion, energy, and pressure are in excellent agreement with the standard RxMC simulations, and all simulations result in a high number (more than 10^6) of accepted forward and reverse reaction steps. The variables shown with an asterisk have been converted to reduced units with respect to the LJ parameters of the R species. The variables ρ_T*, x_P, U*, and P* represent the atomic density of the simulation cell ($(N_R + 2N_P)/V$*), the average mole fraction of species P, the average energy of the simulation, and the average pressure, respectively. The results show that, as the number of replicas increases, the standard deviation of the results tend to increase, and this is consistent with other implementations of the replica exchange technique.[6] Several different combinations of $\delta\kappa$ and $\delta\Delta G_{AB}^\circ$ values have also been tested, and the simulation averages are invariant to the choice of these variables, as well as to the total number of replicas used.

B. Efficiency: High-Density Reacting Mixture. Next, in order to demonstrate the utility of the replica exchange technique, we chose simulation conditions that typically present difficulties for standard Monte Carlo sampling, low temperatures and high densities. In order to quantify the efficiency, we compare the number of MC steps needed to equilibrate the system, as well as the number of accepted forward and reverse reaction steps following the equilibration period. After equilibration, the number of accepted forward and reverse reaction steps should be nearly equivalent. Any observed net drift in the conversion is indicative of a system that is not yet fully equilibrated.

These next simulations were performed at a density of ρ_T* = 0.69 and at a temperature of T* = 3.0 which corresponds to a dense liquid. To aid equilibration, the simulations were first run at an elevated temperature of T* = 10.0 for 100×10^6 MC steps prior to either the RxMC or the RE-RxMC simulations performed at T* = 3.0. As a result, the initial mole fraction of the product in all of these high-density simulations is $x_P = 0.317$, which corresponds to the final configuration taken from the high-temperature equilibration performed at T* = 10.0. To establish a reference with which to compare our RE-RxMC results, two independent simulations were performed using standard RxMC simulations for a total of $10\,000 \times 10^6$ MC steps. The results from these two simulations were then averaged together, in order to generate improved results. The instantaneous mole fraction of the product (x_P) is plotted in Figure 1 as a function of the number of Monte Carlo steps. It is obvious from the figure that these conditions require a significant equilibration period, and even after equilibration, the sampling is still relatively poor (i.e., very few forward and reverse reaction steps are accepted and there are strong correlations present). However, if equilibrium is assumed to be reached at 3000×10^6 MC steps, then the average mole fraction of P is calculated to be 0.225 ± 0.010.

In the previous set of simulations (performed at high temperature and low density), the performance of the RE-RxMC

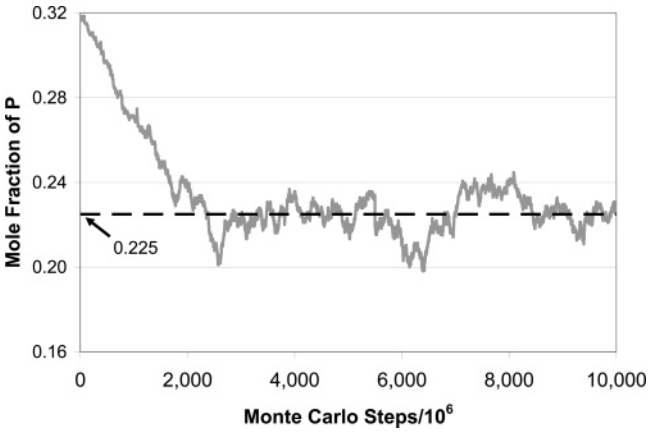

Figure 1. Instantaneous mole fraction of P (solid gray line) versus the number of Monte Carlo steps using traditional RxMC simulations and the average mole fraction of P (dashed black line).

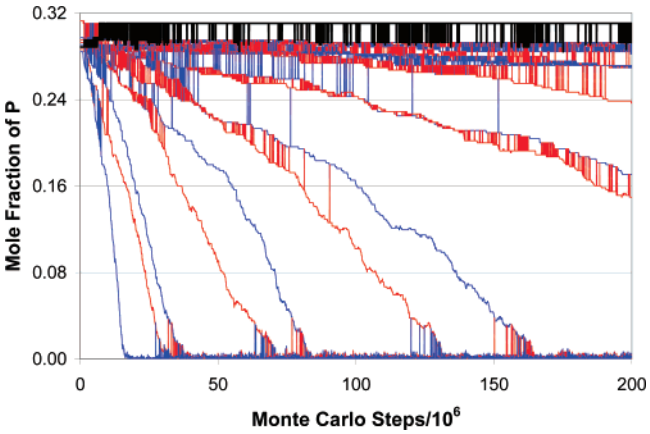

Figure 2. RE-RxMC simulation results at $T^* = 3.0$ and $\rho_T^* = 0.69$ with $\delta\kappa = -0.03$, $\delta\Delta G_{AB}^\circ = 0$, and $M = 19$. The central replica is shown in black, and the neighboring images are shown as alternating red and blue lines.

technique was consistently accurate and efficient, regardless of the details of the replica exchange parameters. At these previous conditions, equilibration is always rapid, and the average system properties can be quickly estimated. However, at the low temperature and high-density condition, the particular choice of the replica exchange parameters have a much greater impact. In the following, we discuss the procedures that result in satisfactory replica exchange performance, as well as several alternatives that yield poor performance, for our particular system. We find that while different procedures affect the efficiency of the RE-RxMC technique, the accuracy of the simulation results is unaffected.

In the first set of simulations, only the potential energy was scaled, so that $\delta\Delta G_{AB}^\circ = 0$ among all of the replicas (as was done for the low density and high-temperature simulations reported in section 4.A). Several different values of $\delta\kappa$ were tested, ranging from -0.01 to -0.10, and different numbers of replicas were incorporated, ranging from 1 to 50. However, regardless of the particular $\delta\kappa$ and M values used, the resulting performance was poor. In the case where $\delta\kappa$ is small (-0.01), then the last replica with the softest potential is still not able to accept many forward and reverse reaction moves, since the last replica is still not very soft (using a moderate number of replicas: $M < 30$). Thus, the benefits of the replica exchange technique are lost. In the case where $\delta\kappa$ is large (-0.10), then the conversions of the neighboring replicas become substantially different, and the acceptance rates for replica exchange moves become vanishingly small. As an example, Figure 2 shows the RE-RxMC results with parameters $\delta\kappa = -0.03$, $\delta\Delta G_{AB}^\circ = 0$ and $M = 19$. The conversions within the replicas deviate significantly from the central image, resulting in wasted replicas and simulation effort. Successful exchanges during the simulation can be identified as vertical jumps among the alternating red and blue lines, and successful exchanges quickly diminish as the replicas begin to deviate from the central image. Alternately, if temperature is used as the sole index parameter among the replicas rather than the interaction parameter ($\delta\kappa$), a similar situation occurs. If the temperature increment is small, then the sampling at the highest temperature replica is only marginally better than within the central replica, and if the temperature increment is large, then large differences in the concentrations among the replicas are present (similar to Figure 2), resulting in low swap efficiency.

In our second set of simulations, we combined the $\delta\kappa$ scaling with the $\delta\Delta G_{AB}^\circ$ scaling to improve the replica exchange performance. Ideally, we would like the conversions of all of the replicas to overlap the central image. However, since the equilibrium conversion of the central image is typically not known a priori, there is not a clear choice for the $\delta\Delta G_{AB}^\circ$ scaling. Therefore, we performed a set of simulations with different values of $\delta\Delta G_{AB}^\circ$, to determine the sensitivity of the results to this parameter. In the best case scenario, we may be able to approximate the conversion of the central image from some previous experimental or simulation data, or we simply may need to make a good first guess. This estimate may also be obtained by assuming an appropriate equation-of-state and approximating the conversion of the reaction at the given state conditions. Regardless, in this particular case, the (lengthy) standard RxMC simulations predict a mole fraction of P of approximately 0.225. Therefore, this serves as our target for scaling the $\delta\Delta G_{AB}^\circ$ value in our first RE-RxMC simulation attempt. To test the robustness of the RE-RxMC approach, we also performed simulations in which we choose values considerably different: $x_P = 0.278$ and $x_P = 0.161$. Although these are poor choices, we find that the average mole fraction of P in the central replica is still predicted accurately, albeit with longer equilibration times needed. Moreover, we show later that it is possible to quickly identify these mole fractions as poor guesses by examining some preliminary simulation output.

Alternately, we may instead start the replica exchange procedure immediately after a standard RxMC simulation (perhaps at a slightly lower density or higher temperature at which chemical equilibrium can be well-determined), thereby establishing an estimate target composition of the system, yet significantly increasing sampling efficiency from that point onward. One possible prescription is as follows. Our RE-RxMC simulations are preceded by two very short RxMC simulation runs. First, we begin by choosing a value of κ that allows a significant number of forward and reverse reaction steps (at least 10^6 during the course of the simulation), which from test simulations at our particular reacting conditions was found to be $\kappa \leq 0.70$. Here, we specifically use $\kappa = 0.64$. We then run a preliminary standard RxMC simulation ($M = 1$) with this value of κ and tune the value of ΔG° until the conversion in the simulation matches our approximate composition target (here, $x_P = 0.225$). This is a short simulation requiring less than 10×10^6 MC steps. The simulation will follow the standard RxMC acceptance rules for forward and reverse reaction steps, which can be written in terms of the standard free energy of the reaction:

$$P_{acc} = \min\left[1, \exp(-\beta\Delta U)\exp(-\xi\Delta G^{\circ}/RT)\prod_{i=1}^{C}\left(\frac{P^{\circ}V}{RT}\right)^{\xi\nu_i}\prod_{i=1}^{C}\frac{N_i!}{(N_i+\xi\nu_i)!}\right] \quad (24)$$

Once the shifted value of ΔG° has been obtained (here, $\Delta G^{\circ\prime} = -15.0$), we then have two reference cases ($\kappa = 1.0$ with $\Delta G^{\circ} = -25.0$ and $\kappa = 0.64$ with $\Delta G_M^{\circ} = \Delta G^{\circ\prime} = -15.0$). The values of ΔG_i° for the intermediate replicas are simply linear interpolations between these two cases, so that the free energy difference between neighboring replicas differ by $\delta\Delta G_{AB}^{\circ} = (\Delta G_M^{\circ} - \Delta G_1^{\circ})/(M-1)$. Likewise, κ differs between neighboring replicas by $\delta\kappa = (\kappa - 1.0)/(M-1)$.

After the initial tuning stage is complete, we then use this value of $\Delta G^{\circ\prime} = -15.0$ and $\kappa = 0.64$ to generate (again using a standard RxMC simulation) a configuration reservoir to be used later in the RE-RxMC simulations. This reservoir is populated by periodically saving configurations from a single RxMC simulation lasting 150×10^6 MC steps. Although this reservoir is not a requirement in the RE-RxMC algorithm, it significantly increases the efficiency of the simulations. Equilibration is greatly enhanced since this allows exchanges to be performed from an already converged Boltzmann ensemble during the RE-RxMC simulation. In this way, at the very beginning of the simulation, the correct ensemble is already available within the last replica (i.e., the reservoir), reducing the overall equilibration time required. As a side note, we have tested different sized image reservoirs (ranging from 2000 to 10 000 configurations) in the RE-RxMC simulations, and the results are unaffected.

After following this two-step initialization procedure, the RE-RxMC simulation was then performed using the initial composition target of $x_P = 0.225$, along with the parameters $\delta\kappa = -0.03$, $\delta\Delta G_{AB} = 0.83$, and $M = 13$. The instantaneous value of x_P in the central image is shown in Figure 3, along with the values from the standard RxMC simulations. This scheme allows the central image to rapidly approach its global minimum, and the total number of accepted forward and reverse reaction steps is increased by almost four orders of magnitude (1.5×10^6 vs 130 per 1000×10^6 MC steps) because of efficient configuration swaps with neighboring replicas.

The efficiency of the RE-RxMC approach can be adversely affected when a poor choice is made for the initial composition target. In the next test, we used an initial composition target of $x_P = 0.278$ with replica exchange parameters of $\delta\kappa = -0.03$, $\delta\Delta G_{AB}^{\circ} = 1.08$, and $M = 13$. The instantaneous value of x_P in the central image is shown in Figure 4, along with the values from the RxMC simulations. While the RE-RxMC simulation took longer to equilibrate ($\sim 4000 \times 10^6$) when compared with the standard RxMC simulations ($\sim 3000 \times 10^6$), after equilibration, the sampling is significantly better, as quantified by a dramatic increase in the number of accepted forward and reverse reactions steps. Most importantly, the average mole fraction of P is unaffected by the poor initial guess of the equilibrium conversion. A summary of these results is included in Table 3, where # MC_{equil} is the approximate number of Monte Carlo steps needed to equilibrate the system and # rxns is the total number of forward and reverse reactions accepted after the initial equilibration period.

In the next test, we used an initial composition target of $x_P = 0.161$ with similar replica exchange parameters: $\delta\kappa = -0.03$, $\delta\Delta G_{AB}^{\circ} = 0.58$, and $M = 13$. However, these parameters resulted in low acceptance probabilities for the replica exchange moves because of poor overlap among the replica Hamiltonians. The reason for the poor overlap is not clear, but it may be related to the direction of approach toward the equilibrium. In this case, the mole fraction of P must increase to reach the equilibrium conversion, which may present more of a sampling challenge. To compensate for this, we increased the total number of replicas from 13 to 23 (including the central image) and performed the necessary modifications to $\delta\kappa$ and $\delta\Delta G_{AB}^{\circ}$, as listed in Table 3. The results from this test are shown in Figure 5, along with the previous results from the standard RxMC simulations. Again, because of the poor initial guess, this RE-RxMC simulation took longer to equilibrate ($\sim 4000 \times 10^6$) when compared with the standard RxMC simulations ($\sim 3000 \times 10^6$), but after equilibra-

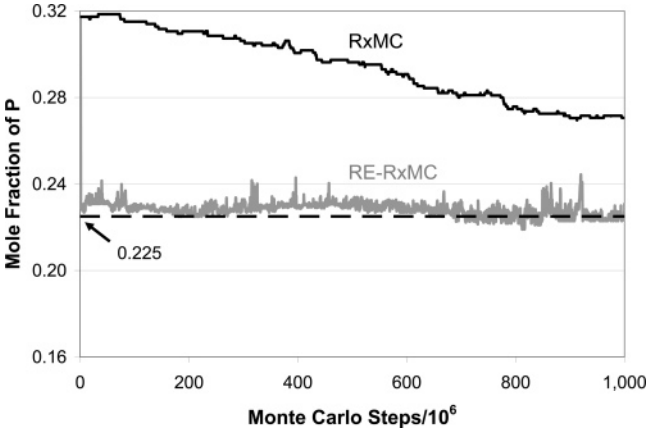

Figure 3. RxMC versus RE-RxMC simulation results at $T^* = 3.0$ and $\rho_T^* = 0.69$ with $\delta\kappa = -0.03$, $\delta\Delta G_{AB}^{\circ} = 0.83$, and $M = 13$. For clarity, only the central replica is shown (solid gray line), along with the average mole fraction from the standard RxMC simulations (dashed black line) for comparison. The initial target composition is $x_P = 0.225$.

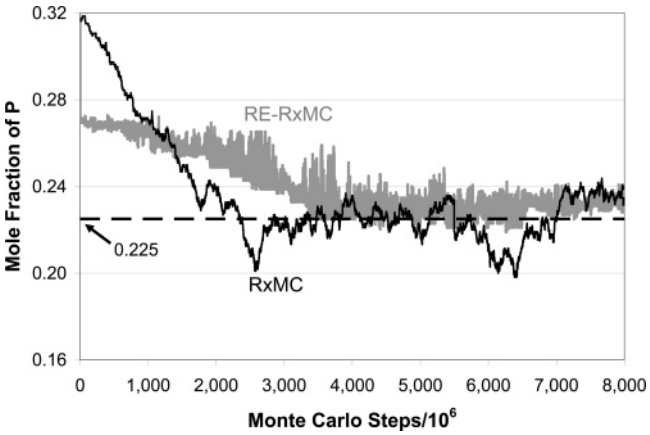

Figure 4. RxMC versus RE-RxMC simulation results at $T^* = 3.0$ and $\rho_T^* = 0.69$ with $\delta\kappa = -0.03$, $\delta\Delta G_{AB}^{\circ} = 0.83$, and $M = 13$. For clarity, only the central replica is shown (solid gray line), along with the mole fraction (solid black line) and average mole fraction (dashed black line) from the standard RxMC simulations for comparison. The initial target composition is $x_P = 0.278$.

TABLE 3: Efficiency of the Replica Exchange Technique against Standard RxMC Simulations for the Reaction 2R ↔ P

M	δk	$\delta\Delta G_{AB}^{\circ}$	x_P (target)	x_P (calculated)	# $MC_{equil}/10^6$	# rxns
1				0.225(10)	~3,000	130
23	−0.016	0.318	0.161	0.221(3)	~4,000	1.4×10^6
13	−0.030	0.830	0.225	0.228(2)	~150	1.5×10^6
13	−0.030	1.080	0.278	0.230(2)	~4,000	8.3×10^6

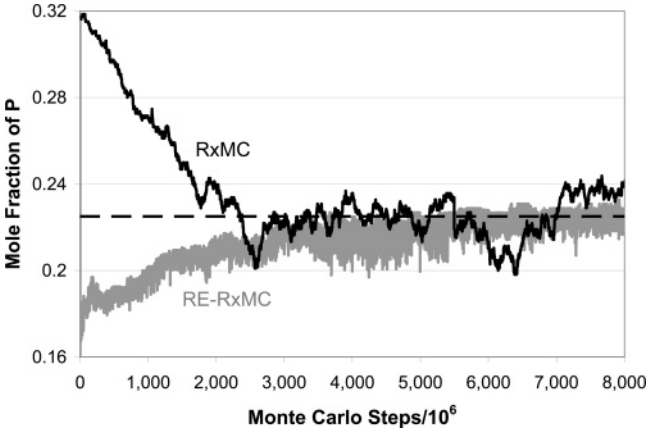

Figure 5. RxMC versus RE-RxMC simulation results at $T^* = 3.0$ and $\rho_T^* = 0.69$ with $\delta\kappa = -0.016$, $\delta\Delta G_{AB}^\circ = 0.318$, and $M = 23$. For clarity, only the central replica is shown (solid gray line), along with the mole fraction (solid black line) and average mole fraction (dashed black line) from the standard RxMC simulations for comparison. The initial target composition is $x_P = 0.161$.

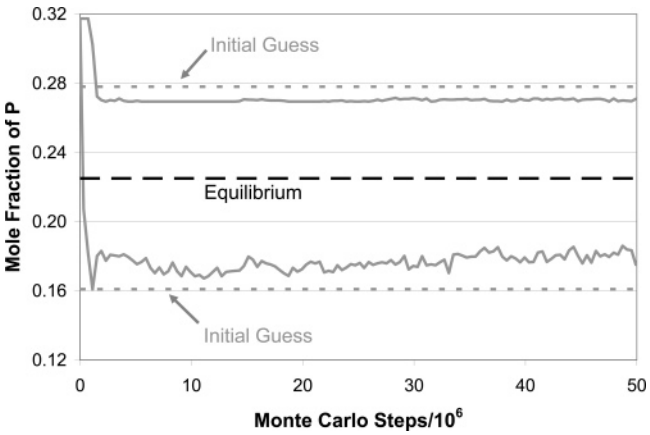

Figure 6. Initial behavior of the RE-RxMC simulations at $T^* = 3.0$ and $\rho_T^* = 0.69$ with guesses of $x_P = 0.161$ and $x_P = 0.278$. For clarity, only the results from the central image are shown (solid gray lines) along the initial guesses (dashed black lines). Both simulations immediately deviated from the initial guesses toward the global minimum.

tion, the sampling is significantly better. As with the previous test, the average mole fraction of P is unaffected by the poor initial guess of the equilibrium conversion. The results from this simulation are also included in Table 3 for comparison.

After performing several tests with the RE-RxMC technique, we conclude that a good guess for the initial target composition, although not mandatory, significantly reduces the equilibration time. We stress here that post-equilibration sampling efficiency is consistently improved when the RE-RxMC method is applied. Therefore, it would be beneficial to be able to quickly identify poor guesses, so that excessive equilibration time is avoided. This can be accomplished by examining the initial behavior of the system from short RE-RxMC simulations. If the initial guess is poor, we find that the system will immediately begin drifting away from this value toward the true equilibrium composition of the system. If the initial guess of x_P is fairly accurate, then the central image will merely fluctuate near the initial guess. To demonstrate this, the initial results from the RE-RxMC simulations with guesses of $x_P = 0.161$ and $x_P = 0.278$ are shown in Figure 6 along with the initial guess. Even at very short times, the central replica immediately departs from the initial guess toward the true equilibrium value, and this behavior is consistently observed for other poor initial guesses, as well.

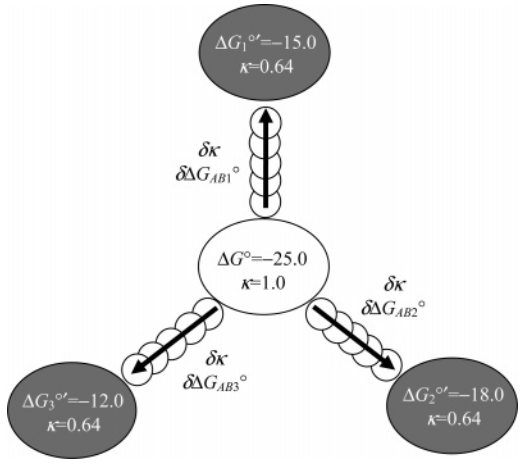

Figure 7. Diagram of the RE-RxMC technique using multiple reservoirs. Here, three reservoirs are used (shaded in gray), where each reservoir is constructed from a standard RxMC simulation with a scaled potential and a different value of $\Delta G^{\circ\prime}$.

Although this analysis cannot be used to predict the expected value of the equilibrium conversion, it provides immediate feedback with regards to the quality of the initial guess.

One simulation scheme that may help minimize the need for a good initial guess is the incorporation of multiple reservoirs. For instance, multiple guesses can be simultaneously incorporated by pregenerating several configuration reservoirs, spanning a range of system compositions. Replica exchange moves can then be performed between the central image and the replicas which lead toward the multiple pregenerated reservoirs, as illustrated in Figure 7. In this figure, three different reservoirs are used, and each of these reservoirs is generated in a standard RxMC simulation by assuming a different equilibrium conversion. For our particular reaction, we have tested this approach by incorporating our three previous guesses for the product mole fraction ($x_P = 0.161$, 0.225, and 0.278), which correspond to $\Delta G^{\circ\prime} = -12.0$, -15.0, and -18.0. A total of 16 replicas connect the central image to each of the preconverged reservoirs, resulting in a total of 49 images (1 central image + 3 × 16 replicas).

The results from the multi-reservoir RE-RxMC simulation are shown in Figure 8. For clarity, only the mole fraction of the central image is shown. As anticipated, the central image is able to very quickly identify (within this composition range) the equilibrium conversion of the system. Moreover, the approach to equilibrium is not deterred when the poor mole fraction reservoirs are incorporated ($x_P = 0.161$ and 0.278), and a large number of forward and reverse reaction steps are accepted following the brief equilibration period. As compared with the previous RE-RxMC simulations reported in Table 3, the multi-reservoir simulation required $\sim 450 \times 10^6$ MC steps for equilibration (since 3 distinct reservoirs must be pregenerated from separate RxMC simulations), the average mole fraction is $x_P = 0.235$, and the total number of reactions accepted in the central image following the equilibration period is 1.4×10^6 per 1000×10^6 MC moves. Although more time is initially required to generate the reservoirs, the multi-reservoir scheme broadens the overall sampling scheme, allowing the central image greater flexibility and ultimately leading to more rapid equilibration. However, since many replicas are involved in this multi-reservoir approach, the total number of forward and reverse reaction moves accepted in the central image is somewhat diluted. This could be improved by pruning the replicas leading to the reservoirs with poor choices of x_P,

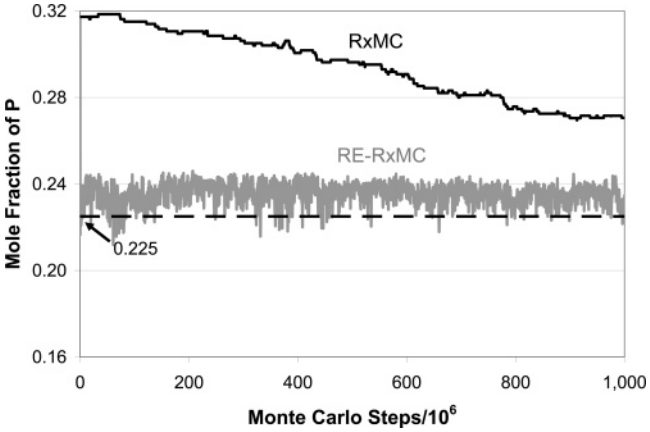

Figure 8. RxMC versus RE-RxMC simulation results at $T^* = 3.0$ and $\rho_T^* = 0.69$ with multiple reservoirs ($x_P = 0.161$, 0.225, and 0.278), corresponding to the diagram shown in Figure 7. A total of 16 replicas connect the central image to each of the reservoirs. For clarity, only the central replica is shown (solid gray line), along with the mole fraction (solid black line) and average mole fraction (dashed black line) from the standard RxMC simulations for comparison.

immediately after the reservoir closest to the equilibrium conversion is identified.

5. Conclusions

In our study, we have developed the acceptance rules for combining the replica exchange technique with standard RxMC simulations. Our results demonstrate that this new RE-RxMC simulation approach is a reliable method for predicting chemical equilibrium and can be used to accelerate standard RxMC simulations at computationally challenging conditions. Furthermore, our results suggest that there are several important considerations that should be made when conducting RE-RxMC simulations. First, scaling only one of the system parameters (such as the temperature or the potential energy) may lead to low acceptance probabilities during the replica exchange steps because of poor configurational overlap between neighboring replicas. The overlap may be enhanced by combining a scaled potential energy with scaled values of the reaction free energy, thereby mitigating dramatic shifts in the equilibrium conversion among the replicas. In addition, from preliminary simulations, we found that incorporating a preconverged structure reservoir as the last reservoir, instead of simulating this reservoir on-the-fly, can significantly enhance convergence. Most importantly, even when a poor choice is made for this preconverged reservoir, the results from the simulations are still reliable. However, the simulations proceed much more efficiently when the reservoir is generated close to the equilibrium conversion of the central replica, and we highlight one approach for quickly eliminating poor initial guesses. Also, we have explored a multiple reservoir method for enhancing the RE-RxMC simulations. Although additional effort is required prior to the equilibration period to generate the multiple reservoirs, the method significantly reduces the equilibration period when a good estimate of the conversion cannot be made a priori.

Our results suggest that the RE-RxMC method is a candidate solution for dealing with equilibrium reactions at non-ergodic conditions. However, because of the algorithm complexity, it should be reserved for challenging cases, in which more straightforward, alternative approaches fail to be effective.[28] Also, implementation of this method will likely become challenging as the number of reactions considered in the simulation increases, since additional reactions will increase the parameter space which needs to be explored in the replicas. For instance, the reservoir generation may become tedious in certain cases of multiple reactions. Assuming that approximately 10 reservoirs could adequately span 0 to 100% conversion for a given reaction, then the number of reservoirs required for a completely blind RE-RxMC approach would be 10 $\times$ (# of reactions). However, if poor sampling in a standard RxMC simulation containing multiple reactions can be attributed to a particular reaction, then the relevant parameter space may be significantly reduced in a RE-RxMC simulation.

Our RE-RxMC simulation approach is similar in spirit to the parallel excluded volume tempering method used by Vlugt and Dünweg.[38] These authors used a grand canonical Monte Carlo approach to predict phase equilibria for single components and binary mixtures. In their procedure, they also soften the intermolecular potential in the replicas (in order to increase the number of successful insertions and deletions) and simultaneously alter the chemical potentials of the components. The modification to the chemical potentials helps mitigate significant compositional variation among the replicas, increasing swap efficiency. This is similar to the logic that we have used for altering the value of ΔG_i° among the replicas.

The RE-RxMC simulations may possibly be enhanced further by pursuing a variety of other options. For instance, the swap efficiency may be enhanced by a more judicious choice of replica parameter spacing. An exchange efficiency of between 20 and 40% has been suggested by others as an optimal target,[35,36,39] but we have not yet attempted to tune the spacing. Also, other general strategies should also be applicable to the RE-RxMC simulations, such as the all-pairs exchange method of Brenner and co-workers.[40] This method was shown to increase simulation efficiency by as much as five times, and it becomes more efficient as the total number of replicas increase.

Acknowledgment. CHT acknowledges support from the UA Research Advisory Council, the Simmons Endowed Excellence Fund, DOE-EPSCoR (DE-FG02-01ER45867), and supercomputing resources provided by an allocation from the NRAC TeraGrid. M.L. acknowledges the Grant Agency of the Czech Republic (Grant 203/05/0725) and by the National Research Programme "Information Society" (Project Nos. 1ET400720507 and 1ET400720409).

References and Notes

(1) Swendsen, R. H.; Wang, J. S. *Phys. Rev. Lett.* **1986**, *57*, 2607.
(2) Hukushima, K.; Nemoto, K. *J. Phys. Soc. Jpn.* **1996**, *65*, 1604.
(3) Neirotti, J. P.; Calvo, F.; Freeman, D. L.; Doll, J. D. *J. Chem. Phys.* **2000**, *112*, 10340.
(4) Hansmann, U. H. E. *Chem. Phys. Lett.* **1997**, *281*, 140.
(5) Czwartos, J.; Coasne, B.; Gubbins, K. E.; Hung, F. R.; Sliwinska-Bartkowiak, M. *Mol. Phys.* **2005**, *103*, 3103.
(6) Yan, Q.; de Pablo, J. J. *J. Chem. Phys.* **2000**, *113*, 1276.
(7) Calvo, F.; Neirotti, J. P.; Freeman, D. L.; Doll, J. D. *J. Chem. Phys.* **2000**, *112*, 10350.
(8) Andricioaei, I.; Staub, J. E. *Physica A* **1997**, *247*, 553.
(9) Fukunishi, H.; Watanabe, O.; Takada, S. *J. Chem. Phys.* **2002**, *116*, 9058.
(10) Sugita, Y.; Kitao, A.; Okamoto, Y. *J. Chem. Phys.* **2000**, *113*, 6042.
(11) Lyman, E.; Ytreberg, F. M.; Zuckerman, D. M. *Phys. Rev. Lett.* **2006**, *96*,
(12) Johnson, J. K.; Panagiotopoulos, A. Z.; Gubbins, K. E. *Mol. Phys.* **1994**, *81*, 717.
(13) Smith, W. R.; Tříska, B. *J. Chem. Phys.* **1994**, *100*, 3019.
(14) Turner, C. H.; Johnson, J. K.; Gubbins, K. E. *J. Chem. Phys.* **2001**, *114*, 1851.
(15) Turner, C. H.; Pikunic, J.; Gubbins, K. E. *Mol. Phys.* **2001**, *99*, 1991.
(16) Turner, C. H.; Brennan, J. K.; Johnson, J. K.; Gubbins, K. E. *J. Chem. Phys.* **2002**, *116*, 2138.

(17) Turner, C. H.; Brennan, J. K.; Pikunic, J.; Gubbins, K. E. *Appl. Surf. Sci.* **2002**, *196*, 366.
(18) Turner, C. H.; Gubbins, K. E. *J. Chem. Phys.* **2003**, *119*, 6057.
(19) Turner, C. H. *J. Phys. Chem. B* **2005**, *109*, 23588.
(20) Turner, C. H. *Langmuir* **2007**, *23*, 2525.
(21) Brennan, J. K.; Lísal, M.; Gubbins, K. E.; Rice, B. M. *Phys. Rev. E* **2004**, *70*,
(22) Lísal, M.; Smith, W. R.; Nezbeda, I. *J. Chem. Phys.* **2000**, *113*, 4885.
(23) Lísal, M.; Brennan, J. K.; Smith, W. R.; Siperstein, F. R. *J. Chem. Phys.* **2004**, *121*, 4901.
(24) Lísal, M.; Smith, W. R.; Bureš, M.; Vacek, V.; Navrátil, J. *Mol. Phys.* **2002**, *100*, 2487.
(25) Lísal, M.; Brennan, J. K.; Smith, W. R. *J. Chem. Phys.* **2006**, *124*.
(26) Lísal, M.; Brennan, J. K.; Smith, W. R. *J. Chem. Phys.* **2006**, *125*.
(27) Smith, W. R.; Lísal, M. *Phys. Rev. E* **2002**, *66*, 011104−1.
(28) Brennan, J. K. *Mol. Phys.* **2005**, *103*, 2647.
(29) Escobedo, F. A. *J. Chem. Phys.* **2001**, *115*, 5642.
(30) Okur, A.; Roe, D. R.; Cui, G.; Hornak, V.; Simmerling, C. *J. Chem. Theory Comput.* **2007**, *3*, 557.
(31) Li, H. Z.; Li, G. H.; Berg, B. A.; Yang, W. *J. Chem. Phys.* **2006**, *125*,
(32) Zuckerman, D. M.; Lyman, E. *J. Chem. Theory Comput.* **2006**, *2*, 1200.
(33) Chase, M. W. *JANAF Thermochemical Tables*, 3rd ed.; American Chemical Society: Washington D.C., 1986.
(34) McQuarrie, D. A. *Statistical Mechanics*, Harper Collins: New York, 1976.
(35) Kone, A.; Kofke, D. A. *J. Chem. Phys.* **2005**, *122*,
(36) Predescu, C.; Predescu, M.; Ciobanu, C. V. *J. Phys. Chem. B* **2005**, *109*, 4189.
(37) Allen, M. P.; Tildesley, D. J. *Computer Simulation of Liquids;* Oxford: New York, 1987.
(38) Vlugt, T. J. H.; Dünweg, B. *J. Chem. Phys.* **2007**, *115*, 8731.
(39) Kofke, D. A. *J. Chem. Phys.* **2002**, *117*, 6911.
(40) Brenner, P.; Sweet, C. R.; VonHandorf, D.; Izaguirre, J. A. *J. Chem. Phys.* **2007**, *126*, 074103−1.